Representing prescribed fire and mechanical thinning in a demographic vegetation model: mechanisms driving forest structure, fuel, and demographic rates in Sierra mixed-conifer forests

Xiulin Gao, Jessica Katz, Charles D. Koven, Adam Hanbury-Brown, and Lara M. Kueppers

The following supporting information is available for this article:

Supplementary methods: Benchmark data and corresponding model metric development

Surface fuels

We compared observed and modeled post-treatment estimates for fine woody debris (FWD) and, where observation data was available, for leaf litter. We did not benchmark 1000-hr fuels, as they are not currently included in the FATES calculation of fire behavior and effects. For Blodgett, we re-analyzed unit-level FWD and leaf litter data collected in 2003, one year following prescribed fire and two years following thinning (Stephens et al. 2025). We used the BerkeleyForestAnalytics package in R (Rutherford et al. 2026) to calculate fuel loads in each treatment. For each fuel class, we constructed a linear model in which fuel load was the response variable and treatment was the covariate. We then calculated the percent difference and associated standard error between the least-squares mean values of the metric in each treatment relative to the control.

For Teakettle, we used PlotDigitizer (Version 3.1.6, 2025) to digitize mean FWD loads (leaf litter data were not available for this site) by treatment for 2003, two years post treatment (North et al., 2009). We then used these previously-reported estimates to calculate the percent difference in fuel load between treatment and control. For STEF, unit- and treatment-level fuel load estimates were not readily available. For this site, we provide a more qualitative evaluation of differences between modeled outputs and reported fuel conditions in 2014 three years post-thinning and one year post-burning from Knapp et al. (2017).

We calculated the FATES-modeled percent difference (and associated standard error) in FWD and leaf litter fuel load between treatment and control using modeled fuel load in 2003 (for thinning) and 2002 (for burning) for Blodgett, 2012 (for burning) and 2014 (for thinning) for STEF, and 2003 (both treatments) for Teakettle. Model outputs have no replicates for each treatment due to the deterministic nature of CLM-FATES, but outputs are calculated on a monthly basis. We therefore calculated the percent difference in treatment relative to the control each month and then calculated the mean and standard error of these differences across months.

Stand structure and composition (stem density, basal area, size distribution, PFT composition):

For each site, we re-analyzed tree-level inventory data, which included observations of diameter and life status collected at multiple timesteps. Due to different site-specific size thresholds for including individuals in inventories, we only included trees whose diameters at breast height (DBHs) were at least 15 cm in our benchmark calculations. We pre-processed tree-level forest inventory data to remove duplicated and null records, harmonize tree species and life status across each tree's re-measurements, and correct typos. We categorized tree species into three PFTs: cedar (incense cedar), fir (including white fir and red fir), and pine (including ponderosa, Jeffrey, and sugar pine). We identified outliers as DBH measurements corresponding to annual growth increments with absolute values exceeding three standard deviations from the site-specific mean DBH increment at each site (Katz et al. *in review*). We replaced the

DBH value(s) associated with outliers with an estimate interpolated from the nearest two measurements in the tree's time series.

For each measurement year and treatment unit, we calculated four metrics from the observations (stem density, basal area, size distribution, and PFT composition). For sites that tracked all trees in each treatment unit (STEF and Teakettle), we calculated stem density as the count of all individuals larger than 15 cm DBH within each unit. Similarly, we calculated the basal area as the sum of the basal areas of all individuals in the unit. Size distribution was the number of individuals within each size class (15-20 cm, 20-30 cm, 30-40 cm, 40-50 cm, 50-60 cm, 60-70 cm, 70-80 cm, 80-90 cm, 90-100 cm, and > 100 cm); and PFT composition was the fraction of total unit basal area comprised by each PFT. At Blodgett, sampling took place within subplots of treatment units. In this case, we calculated metrics at the level of each subplot and then took the mean value across subplots within each unit to estimate the metric at the unit level. For all sites, we normalized the stem density, basal area, and size distribution, and PFT composition by the area of the unit or subplot.

We next used these year- and unit-specific averages to calculate differences between treated and control units. For each treatment unit, we averaged the values of each metric at the beginning and end of each measurement interval; this gave us a series of measurement interval- and unit-specific estimates of each metric. Then, for each measurement interval, we used a linear modelling framework to calculate the least-squares mean value and standard error of each metric across all the units associated with each treatment. In each linear model, the metric (e.g., stem density, basal area) was the response variable, and treatment (Control, Burn, Thin) was the sole covariate. We then calculated the percent difference (and associated standard error based on the delta method) between the mean value of the metric in each treatment relative to the control. Finally, we summarized the metric for the entire post-treatment study period by taking the average of all interval-specific percent differences, weighted by the number of years in the interval. For Teakettle, we modified this process slightly because different treatment units were measured in different years: we calculated unit-specific weighted averages of the metric across all measurement intervals first and then used this study-long average (rather than the interval-specific averages) to estimate the least-squares means, percent differences, and standard errors associated with each treatment.

From the FATES outputs, we calculated analogous percent differences and standard errors between treatment and control for all the four metrics mentioned above. We first calculated the percent difference for each month's output, and then averaged across the study period to calculate the mean percent difference. Standard error was calculated using the monthly percent differences.

As a sensitivity analysis, we also calculated benchmarks based on percent change between the pre-treatment and average post-treatment metrics for each treatment type, which show a similar pattern as the benchmark metrics derived using the relative change approach (see Appendix Figures S2-4).

Demographic rates (growth and mortality)

We benchmarked annual diameter growth increments for trees in each of the size classes listed above. Site- and PFT-specific diameter increments, treatment effects on growth, and 95% credible intervals (95% CI) were estimated using the Bayesian state-space models developed in Katz et al. (*in review*). The effects of mechanical thinning and prescribed burning are expressed as a multiplier on the growth rate estimated for the control; we specifically benchmarked treatment effects for 30-40 cm DBH trees, roughly the median tree size across all post-treatment units.

To calculate the FATES-modeled treatment effect on growth rate, we first calculated the mean annual growth rate per PFT for each year using monthly model outputs for 30-40 cm DBH trees; treatment effect was then calculated by dividing the annual mean growth rate from the treatment by that from the control. With the yearly data, we then calculated the mean treatment effect on growth rate and its 95% CI.

We also compared cumulative mortality rates over the post-treatment study period at each site. We calculated mortality separately for trees between 15 and 60 cm DBH and trees larger than 60 cm DBH. For observed mortality, we used the tree-level inventory data to model the probability of mortality associated with each treatment for each measurement interval at each site using a generalized linear mixed effects model based on a binomial distribution. Treatment was the sole covariate, and unit was a random effect. To estimate the cumulative mortality over the study period, we calculated the survival rate during each measurement interval (one minus the interval mortality rate), and then subtracted the product of the survival rates for all measurement intervals from one.

For FATES-modeled mortality, we first calculated the mean annual mortality (in number of plants per m^2) and mean annual stem density (in number of plants per m^2) per size class by averaging the monthly model outputs for each year and each size class; total mortality per size class per year was then calculated as the sum of mortality across different mortality types (e.g., mortality due to drought or carbon starvation). We then summed the stem density and total mortality for each of the two size groups (15-60 cm and larger than 60 cm) for each year, with this data we then divided the total mortality by total stem density to calculate the annual mortality rate for each size group. Accumulative mortality rate was then calculated as the sum of the annual mortality rate within the observed period for each site and each size group. No standard deviations were calculated.

We estimated all benchmark metrics in R (Version 4.5.2, R Core Team 2025) using the emmeans (Lenth et al. 2024) and lme4 packages (Bates et al., 2015).

References

Bates, D., Mächler, M., Bolker, B. M., and Walker, S. C.: Fitting linear mixed-effects models using lme4, Journal of Statistical Software, 67, 1–48, https://doi.org/10.18637/jss.v067.i01, 2015.

Knapp, E. E., Lydersen, J. M., North, M. P., and Collins, B. M.: Efficacy of variable density thinning and prescribed fire for restoring forest heterogeneity to mixed-conifer forest in the central Sierra Nevada, CA, Forest Ecology and Management, 406, 228–241, https://doi.org/10.1016/j.foreco.2017.08.028, 2017.

Lenth, R., Singmann, H., Love, J., Buerkner, P., and Herve, M.: Package 'emmeans,' R package version, 1, 2024.
Lindeskog, M., Smith, B., Lagergren, F., Sycheva, E., Ficko, A., Pretzsch, H., and Rammig, A.: Accounting for forest management in the estimation of forest carbon balance using the dynamic vegetation model LPJ-GUESS (v4.0, r9710): Implementation and evaluation of simulations for Europe, Geoscientific Model Development, 14, 6071–6112, https://doi.org/10.5194/gmd-14-6071-2021, 2021.

North, M., Innes, J., and Zald, H.: Comparison of thinning and prescribed fire restoration treatments to Sierran mixed-conifer historic conditions, Can. J. For. Res., 37, 331–342, https://doi.org/10.1139/X06-236, 2007.
North, M., Hurteau, M., and Innes, J.: Fire suppression and fuels treatment effects on mixed-conifer carbon stocks and emissions, Ecological Applications, 19, 1385–1396, https://doi.org/10.1890/08-1173.1, 2009.

PlotDigitizer: Version 3.1.6, https://plotdigitizer.com, 2025.

R Core Team: R: A Language and Environment for Statistical Computing, R Foundation for Statistical Computing, Vienna, Austria, https://www.R-project.org/>, 2025.

Rutherford, K., Foster, D., and Battles J.: BerkeleyForestsAnalytics, version 3.0.1. Battles Lab: Forest Ecology and Ecosystem Dynamics, University of California, Berkeley. https://www.google.com/url?q=https://github.com/kearutherford/BerkeleyForestsAnalytics&sa=D&source=docs&ust=1776962617733103&usg=AOvVaw3KTfErDDl3kHP07Rfvr9qc, 2026.

Stephens, S., York, R., Roughton, A., Battles, J., and Collins, B.: The Fire and Fire Surrogate Study: Berkeley Forests, 2001-2020, https://doi.org/10.6073/PASTA/06A3A2556F5289B89B9F8683BECFE08E, 2025.

Supplementary figures

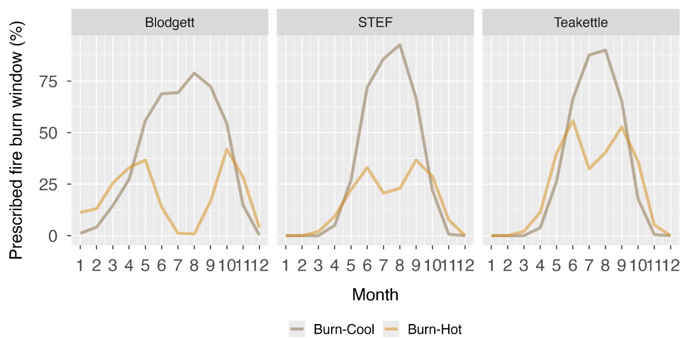

Figure S1. Burn window at each site the two different prescribed fire simulations. Burn-Cool: inclusive burn window; Burn-Hot: exclusive burn window.

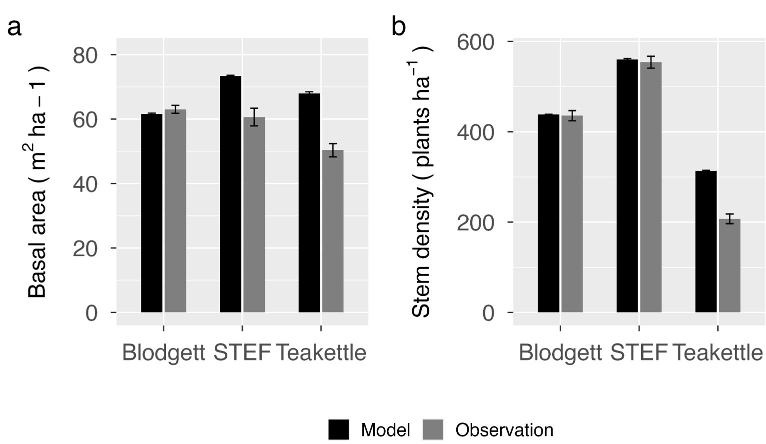

Figure S2. Modeled and observed stand basal area (a) and stem density (b) in the control at the three study sites. CLM-FATES predicted well both the stand basal area (60 - 73 m^2 ha^{-1}) and stem density (310 - 550 plants ha^{-1}) in the control units at Blodgett and STEF (Fig. 4). Both the model-simulated stand density and basal area were about 50% and 40% greater than observations at Teakettle.

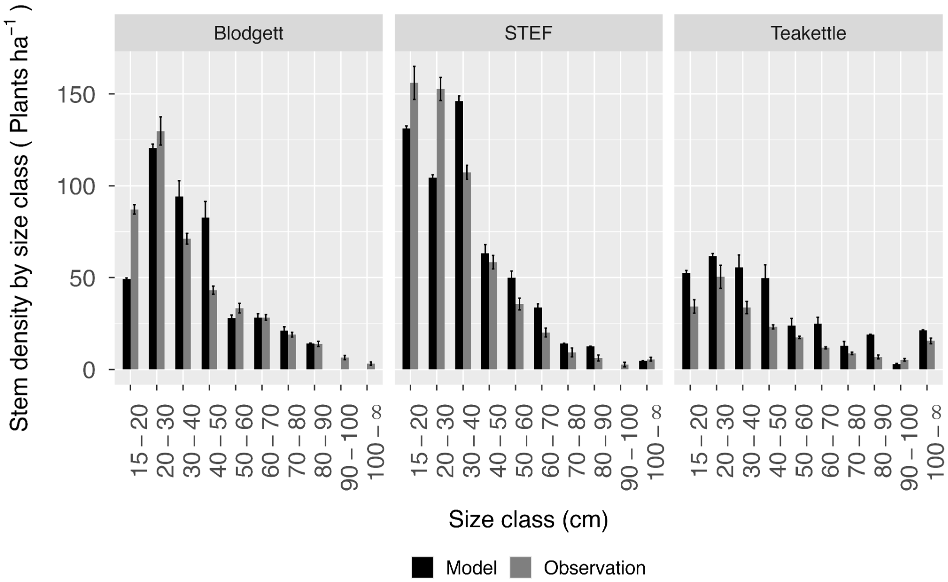

Figure S3. Modeled and observed size structure for the control at three study sites. The simulations of size distribution in the control units reproduced the observed size structure at study sites, though with underestimates of stem density in the smallest size classes at Blodgett and STEF.

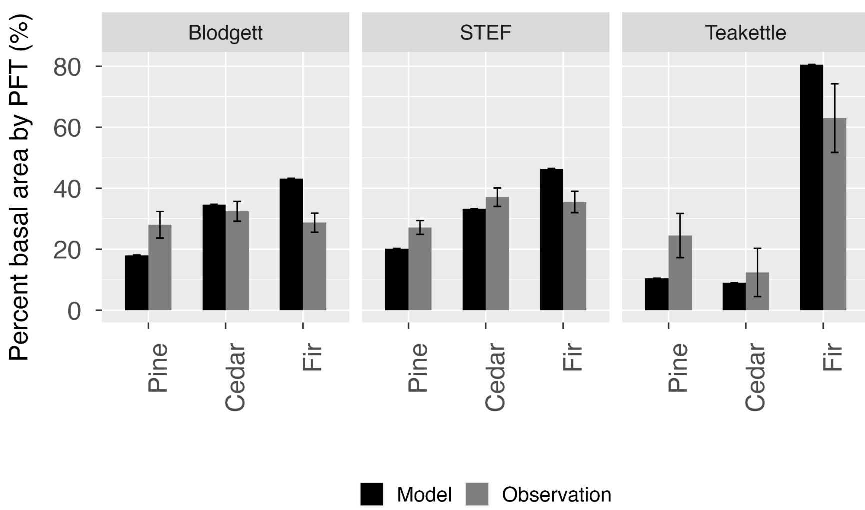

Figure S4. Modeled and observed PFT composition in terms of percent basal area in the control at three study sites. FATES overestimated the basal area of fir in the control by about 5-10%, and underpredicted that of pine by about 10-20% compared to observations. In general, modeled PFT composition predicted a fir-dominated forest type across all three sites, with Teakettle (a cool and wet site in the model) having the highest (~ 80%) and Blodgett (a warm and dry site in the model) having the lowest percent fir by basal area (~ 42%). While this variation in percent fir basal area along the climate gradient was also reflected in the observations, the differences in PFT proportions tended to be smaller in the observations, especially at Blodgett and STEF, where the three conifer PFTs co-dominate the sites.

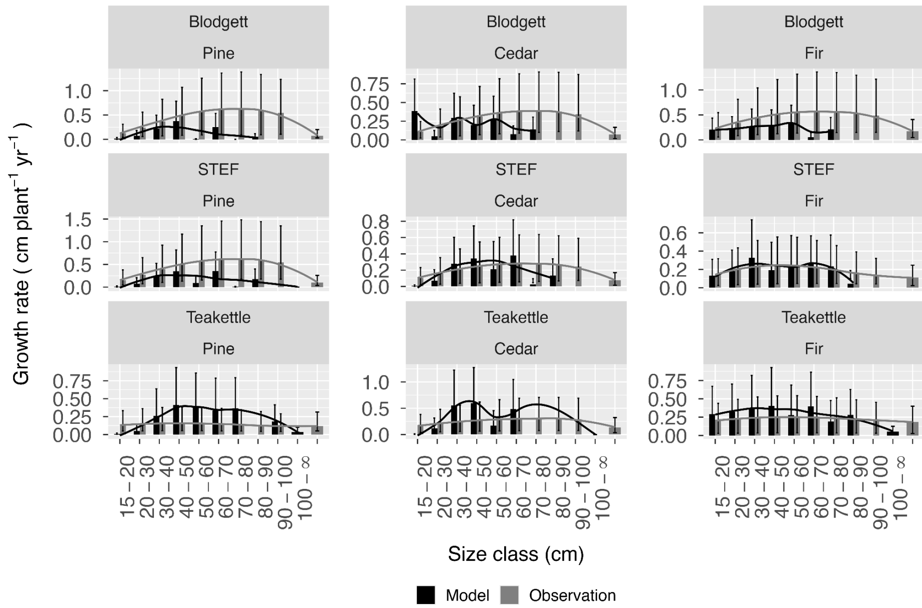

Figure S5. Modeled and observed control growth rate by size class for pine, cedar, and fir PFTs at three study sites. Observed growth rate for each size class is derived using PFT-specific growth models built from growth measurements at each site; pine observations include ponderosa pine and Jeffrey pine but not sugar pine. Error bars indicate the 95% credible intervals. Lines are the locally estimated scatterplot smoothing regressions to show the trend of growth rate as size increases.

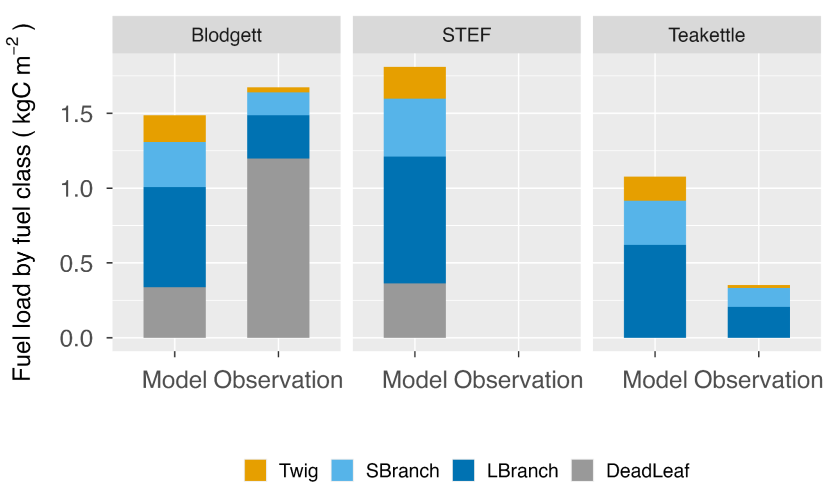

Figure S6. Modeled and observed fuel load in the control by fuel class at three study sites. Leaf litter is not shown for Teakettle because no discrete litter observations are available for this site. The modeled fuel load (1.1 - 1.5 kg C m^{-2}) in the control was either higher (at Teakettle) or slightly lower (at Blodgett) than observed fuel load (0.3 - 1.67 kg C m^{-2}), with the model tending to overestimate FWD, especially 100-hour fuels, but underestimate leaf litter. Differences between the model and observations in fuel load were greatest at Teakettle.

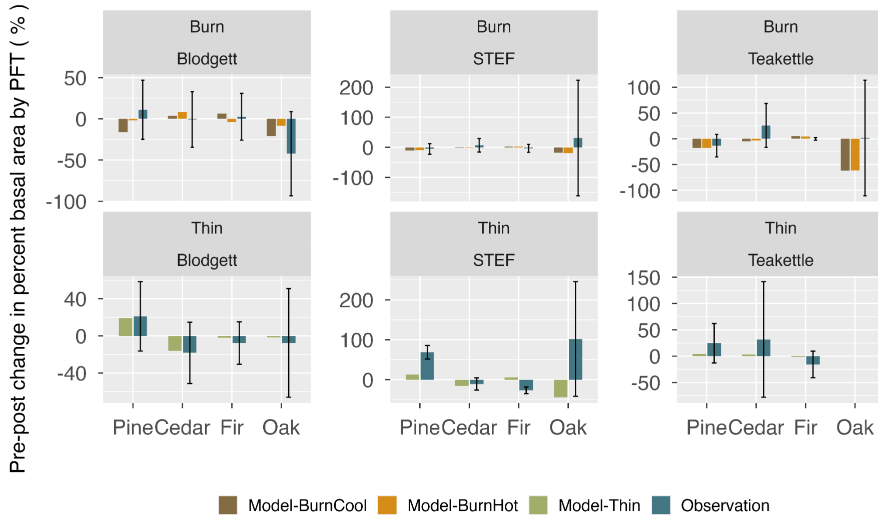

Figure S7. Relative change in percent PFT basal area composition using pre- and post-treatment observations and model data.

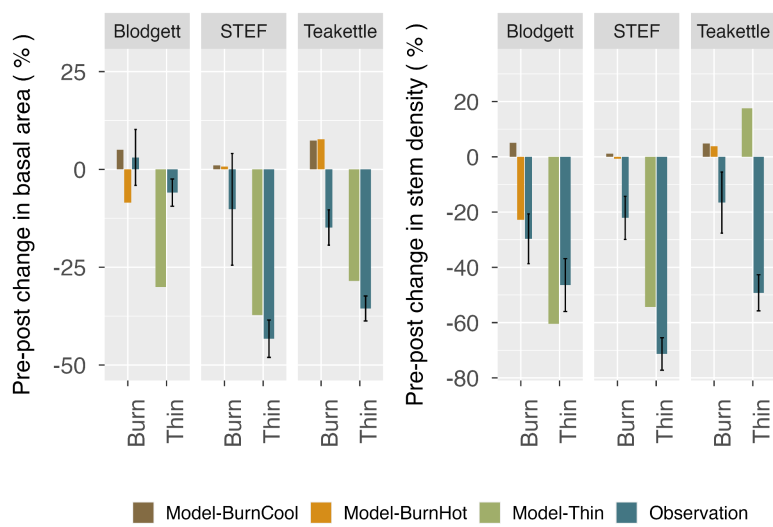

Figure S8. Relative change in basal area and stem density using pre- and post-treatment observations and model data. Model-BurnCool: inclusive burn window; Model-BurnHot: exclusive burn window.

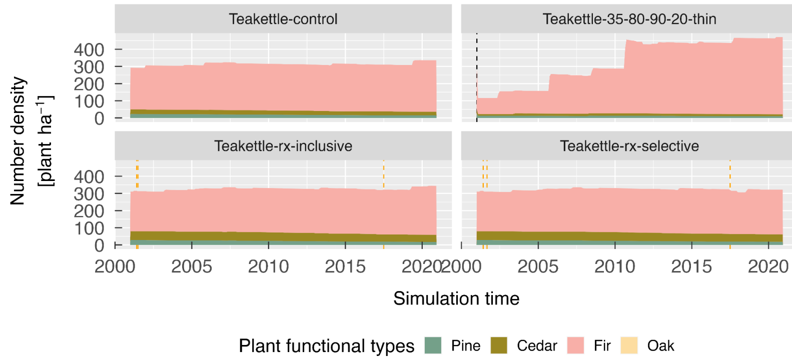

Figure S9. Time series of stem density by each PFT at Teakettle of the control, thinning, and prescribed fire simulations. Black dashed line indicates timing of thinning and orange dashed lines indicates timing of prescribed fires. Notice the increase in fir stem density following thinning at Teakettle.

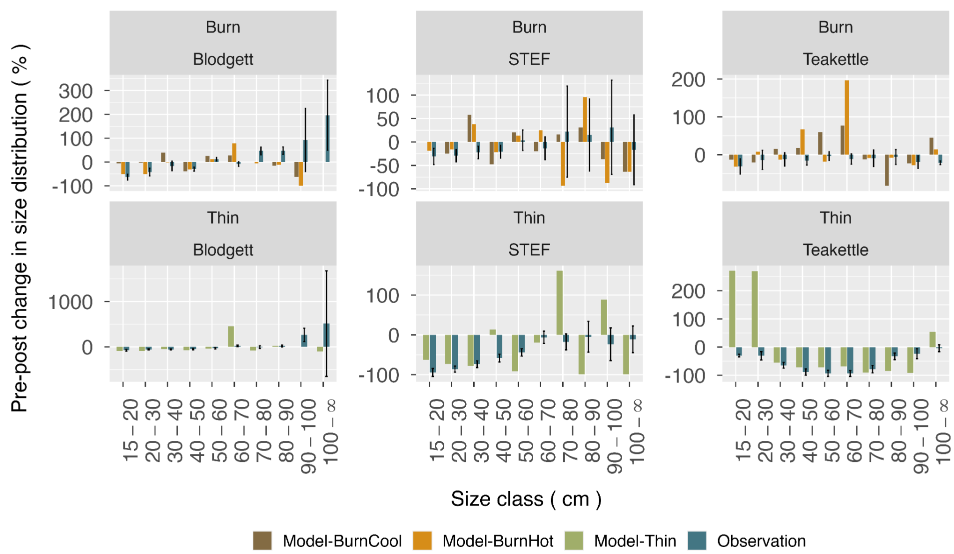

Figure S10. Relative change in stem density by each size class using pre- and post-treatment observations and model data.

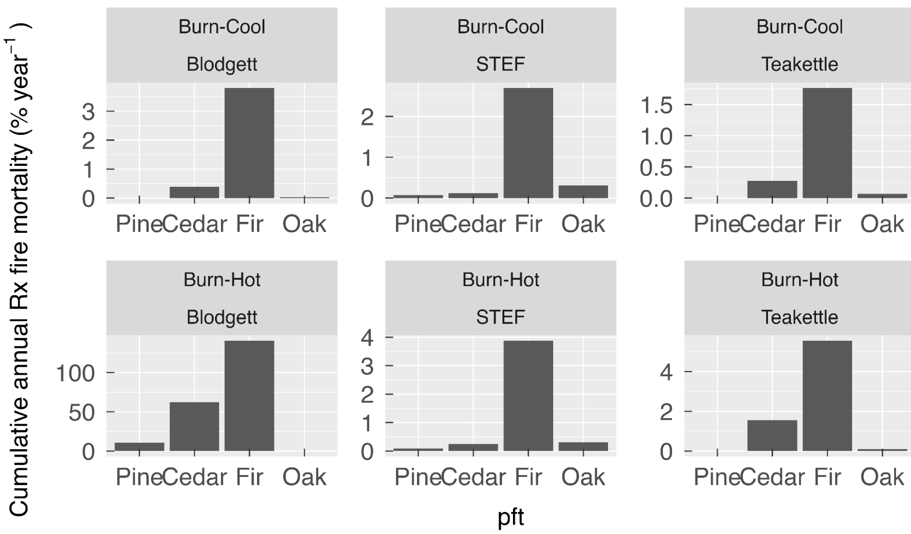

Figure S11. Simulated cumulative annual mean prescribed fire mortality of each PFT at the three sites.

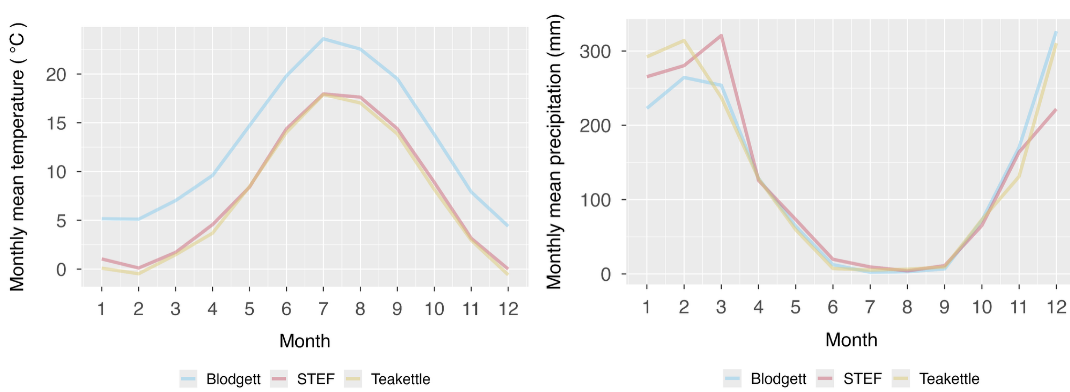

Figure S12. Monthly mean air temperature at 2m above the ground and mean precipitation at each site in the model.